Halfshaft Torque Measurement

Christian Miller

University of Florida Formula SAE

Background

Data on the transient loading through the drivetrain is desired to improve fatigue life estimates of drivetrain and suspension components, and to assist with spring and damper tuning to improve acceleration performance. Loading data from an engine dynamometer is not sufficient since it would not be representative of impact loading and transient conditions. Such conditions are seen often during an autocross course, but are most dramatic when launching from rest.

Introduction

In order to gather transient data while driving on the track, some means of directly measuring torque through the drivetrain components is required. This is accomplished through a torsion bridge applied to the halfshaft to gather loading data from shaft strains. A full torsion bridge is an array of four strain gages wired into a Wheatstone bridge, shown in Figure 1. When this circuit is applied to the halfshaft, its output will directly correspond with the torque that is applied to the half shaft from the engine and transmitted through the suspension and tire.

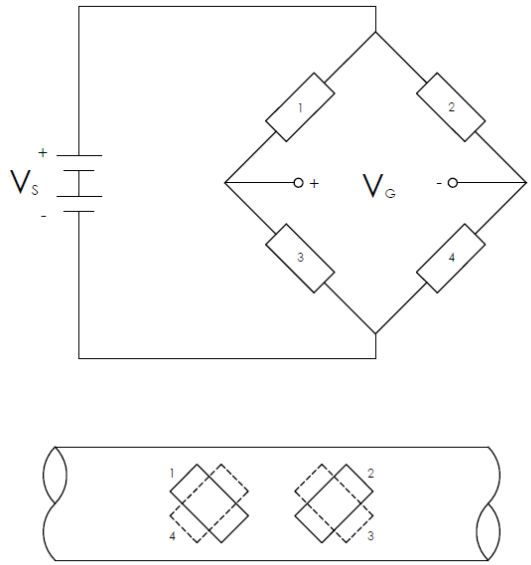

Fig. 1. Torsion Wheatstone Bridge

There are several options for measuring and recording the torsion bridge output. Since the halfshaft is a rotating component, the bridge cannot be directly wired into the vehicle data logger. Two options are to run the bridge through a slip ring to the vehicle data logger, or to use a stand-alone data logger that can be mounted directly onto the halfshaft. Using a slip ring to tie the bridge into the vehicle data logger allows for much easier data synchronization so that multiple vehicle parameters can be analyzed together. However, due to the nature of slip rings, additional noise will be present in the data. Two types of slip rings that can be used for this application are through-bore and end-of-shaft. Through-bore slip rings allow the rotating shaft to pass through the slip ring, allowing measurement in the middle of a shaft, but is considerable more expensive than end-of-shaft slip rings, which as the name suggests, attaches to the end of a shaft. For this particular application, wire routing to an end-of-shaft slip ring is difficult, since it requires routing past the halfshaft bearings, through the center of the hub, and around the outside of the tire.

An alternative is to use a small stand-alone data logger that can be directly attached to the shaft. The wires route directly to the data logger, which is rotating on the shaft with the torsion bridge. This decreases wire routing complexity and the amount of noise present in the signal. It is for these reasons that this method of data logging was chosen. A DTS SLICE NANO system was selected because of its extremely small size (1.0 in x 1.2 in) and mass (~45 grams), and its large load factor rating (500 G's). Refer to [1] for additional specifications. The SLICE NANO system consists of several stackable slices, each with a separate function. For these tests, three slices were used: BASE, BRIDGE and END-OF-CHAIN. This series of slices allow for data logging, Wheatstone bridge connections, data retrieval, event triggering and power supply. Power is supplied via three 9V batteries wired in parallel, which are also attached to the rotating shaft.

Setup

The torsion Wheatstone bridge installed on the halfshaft is shown in Figure 2. Figures 3 and 4 show the experimental setup used in CAD and on the physical vehicle, respectively. The SLICE NANO system is housed in a protective housing to prevent damage due to track debris, as shown in Figures 5 and 6.

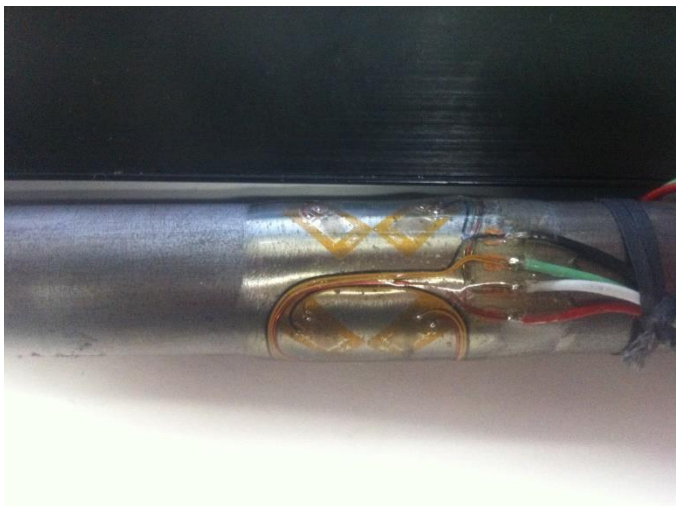

Fig. 2. Torsion Wheatstone Bridge installed on halfshaft

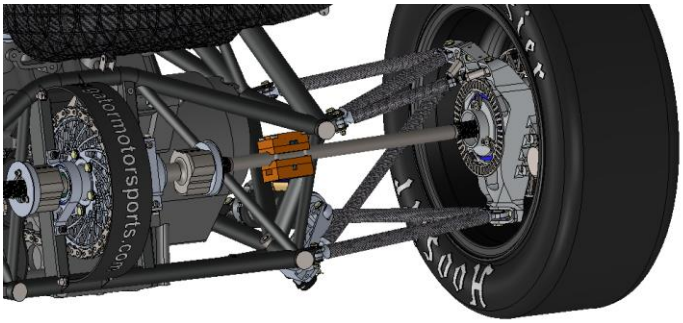

Fig. 3. Experimental Setup in CAD

Fig. 4. Experimental Setup on the Vehicle

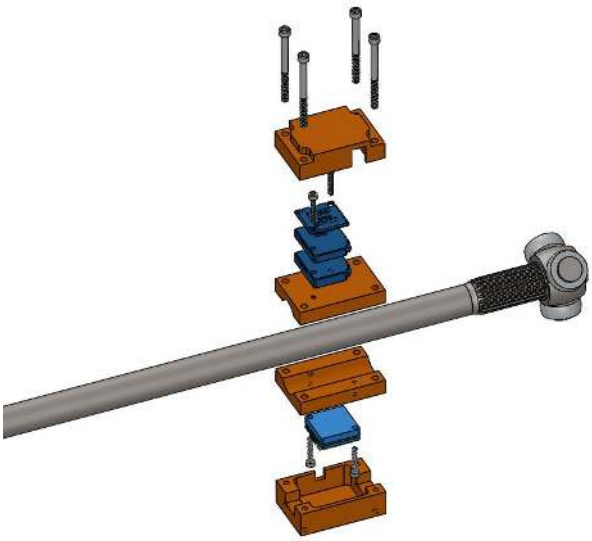

Fig. 5. DTS NANO Assembly in CAD

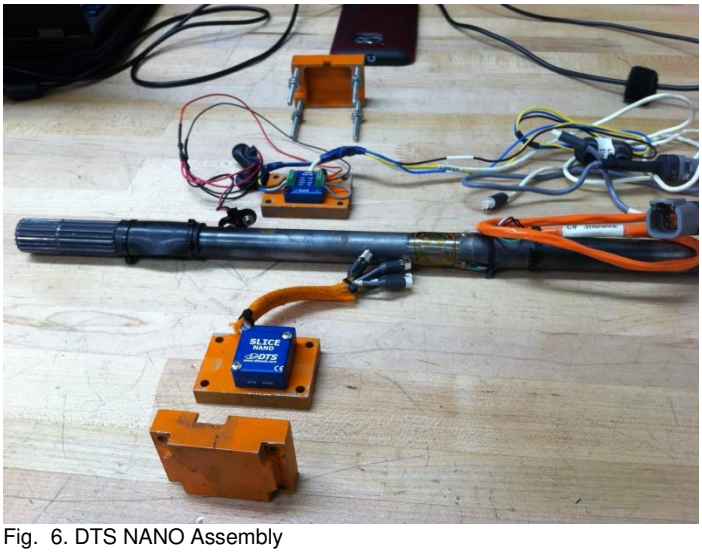

Fig. 6. DTS NANO Assembly

Calibration

Figure 7 shows how the torsion bridge was calibrated. An arm was attached to the hub, and a known weight was suspended at a known distance from the centerline of the hub. From this, the applied torque was calculated and compared to the voltage output from the bridge. A range of torque values were applied and their corresponding voltage outputs were recorded, as shown in Table 1. To account for deflection of the calibration setup due to the applied torque, the angular deflection of the setup was determined, and used as a correction to the applied torque calculation, as shown in Figure 8.

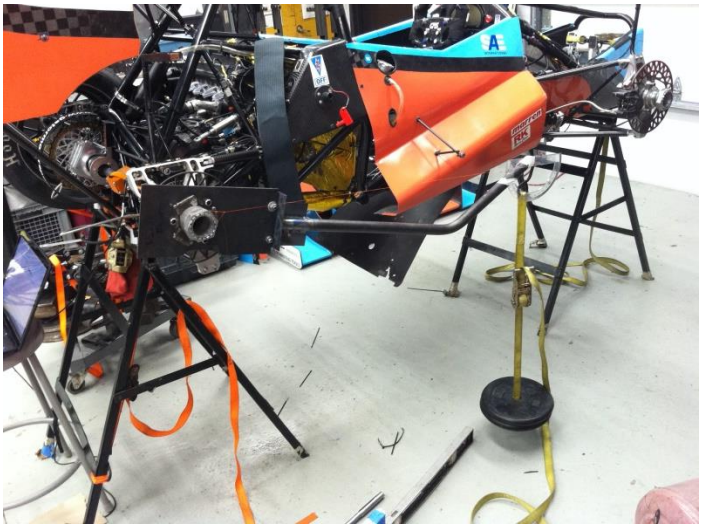

Fig. 7. Torsion bridge Calibration

Fig. 8. Calibration Arm Angular Deflection

TABLE I
TORSION BRIDGE CALIBRATION

Applied Torque (lb-ft)	Bridge Output (mv)
-133.8	-8.132
-73.0	-3.733
-5.4	0.661
0.0	1.030
5.4	1.445
73.4	5.960
136.0	10.436
195.7	14.630

The data in Table I was plotted and a linear fit was made to determine the calibration slope, as shown in Figure 9. The slope of the curve was found to be 0.0687mV/lb-ft. To determine the calibration coefficient to be used, the slope of the curve must be divided by the excitation voltage used when taking the calibration data. An excitation voltage of 5 volts was used, so the calibration coefficient is 0.01374mV/V/lb-ft.

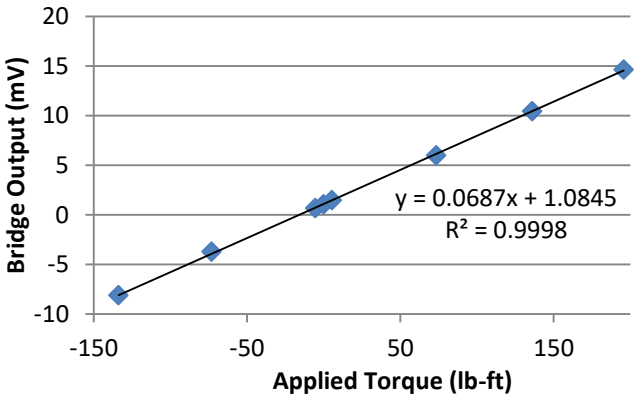

Fig. 9. Torsion bridge Calibration Data

Results

Several sets of data were taken with different tire pressures, spring rates and damper settings, as shown in Table II. Figure 10 shows the axle torque measured during an acceleration run. The data shown in Figure 10 is typical for all sets of data, with minute differences in the amplitude and frequency in the oscillations that are present from zero to two seconds. Figure 11 shows just the traction limited section of the run in Figure 10, where there are the largest differences in between runs. Table III gives statistics about the traction limited section of each set.

TABLE II
VEHICLE SETTINGS

Set	Tire Pressure (psi)	Spring (lb/in)	Damper Setting
1	12	350	Full Soft
2	8	350	Full Soft
3	6	350	Full Soft
4	6	350	Full Stiff
5	6	200	Full Stiff
6	6	200	Full Soft
7	6	550	Full Soft
8	6	550	Full Stiff

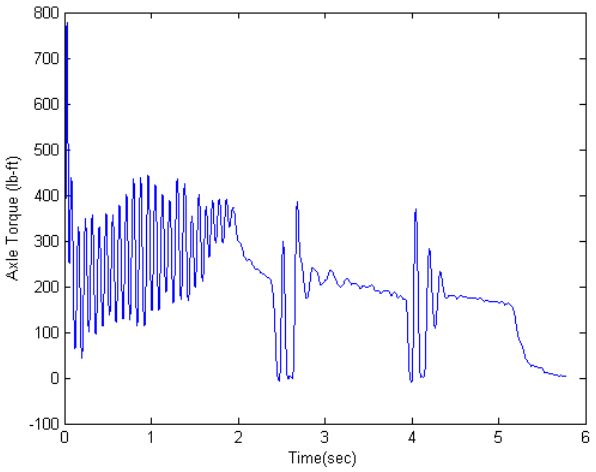

Fig. 10. Axle Torque during Acceleration Run

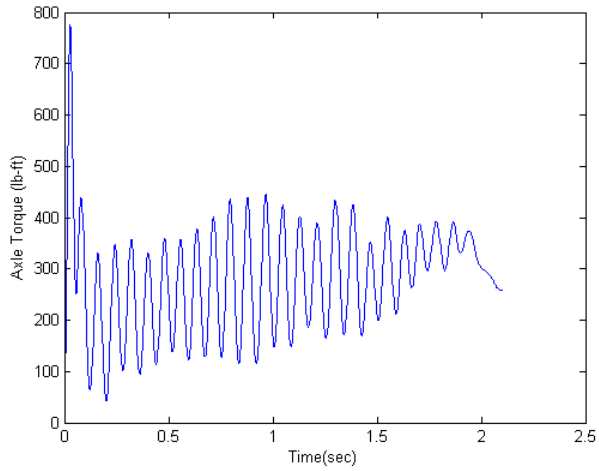

Fig. 11. Axle Torque during Traction Limited Section

TABLE III
TRACTION LIMITED STATISTICS

Set	Area Under the Curve (lb-ft-s)	Standard Deviation (lb-ft)
1	513.0	106.2
2	461.7	109.8
3	476.7	108.5
4	444.1	104.4
5	500.0	116.1
6	448.5	104.4
7	459.5	104.1
8	441.7	109.4

Discussion

The torque measured over time during an acceleration run is show in Figure 10, and is typical of the data gathered for all sets of data. All runs begin with a large spike in torque followed by oscillations that are present for roughly two seconds. An acceleration run can be split into two sections, traction limited and power limited. In the traction limited section of the run, the tractive effort produced by the engine exceeds the available grip at the rear tires, resulting in a large amount of wheel slip. In the power limited section, the available grip at the rear tires exceeds the tractive effort produced by the engine, resulting in low amounts of wheel slip. It has been observed that the oscillations seen in the first two seconds of Figure 10 are present in the traction limited section of the run, and disappear after the transition to the power limited section of the run has occurred.

There is a large variation in the amplitude and frequency of the torque measurement in the traction limited segment, after which the torque measurement is fairly consistent (with the exception of the shift points where the torque measurement spikes). The analysis will be limited to the traction limited section, since that is where the changes in between vehicle settings show the largest variations in the torque measurement. Furthermore, the variation in the location of the shift points in this section of the data would make meaningful analysis difficult.

One measure of evaluating how much torque was “put to the ground” is the area under the torque vs time plot. Table III shows the area under each torque curve taken at a point before the shortest run ended. Since each of the runs remained in the traction limited section of the run for a different period of time, a comparison was made while all runs were still in the traction limited section. This is assumed to be a valid comparison since the slope of the data is steady where the comparison is made, so the result would not change even if all runs lasted the same amount of time. Table V then orders the runs with the set with the largest area under the curve first and set with the least area under the curve last.

A Fast Fourier Transform (FFT) was then performed on the data to compare the frequency content of each run. Figure 12 shows the FFT plots for sets 1-3 to compare the effect of tire pressure. Figure 13 shows the FFT plots for sets 3 and 4 to compare the effect of damper settings. Figure 14 shows the FFT plots for sets 3, 6, and 7 to compare the effect of spring rates with full soft dampers. Figure 15 shows the FFT plots for sets 4, 5, and 8 to compare the effect of spring rates with full stiff dampers.

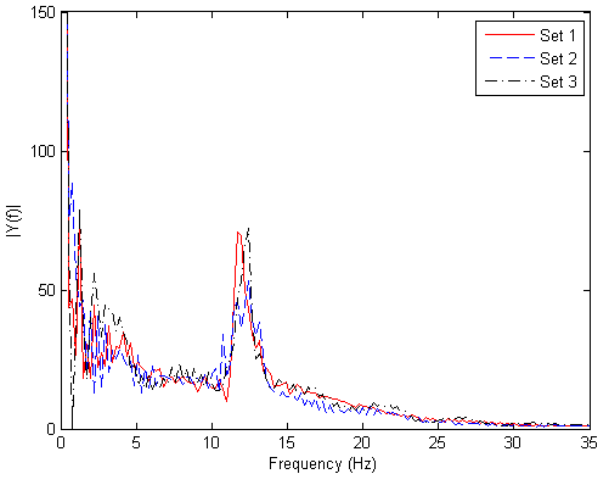

Fig. 12. Sets 1-3 FFT

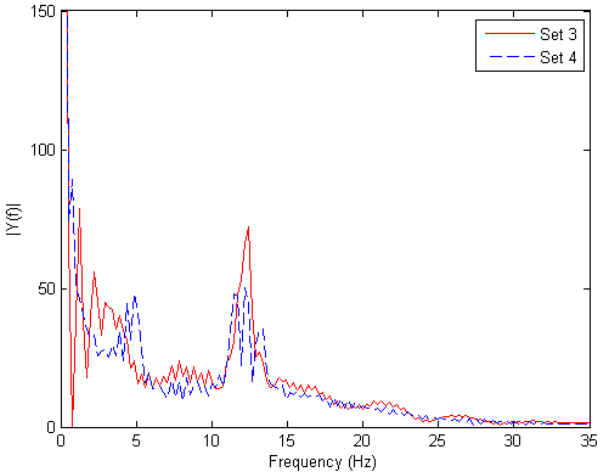

Fig. 13. Sets 3 and 4 FFT

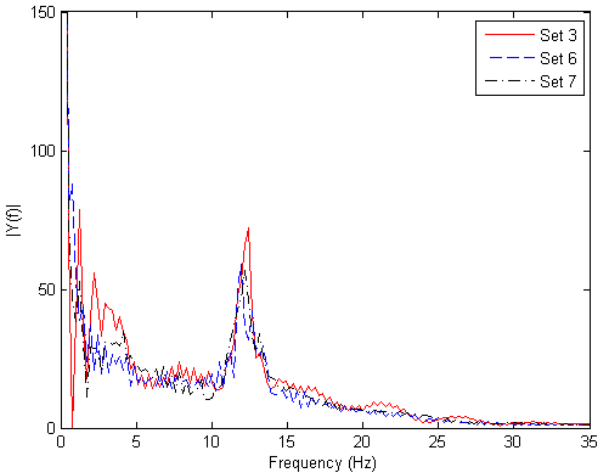

Fig. 14. Sets 3, 6, and 7 FFT

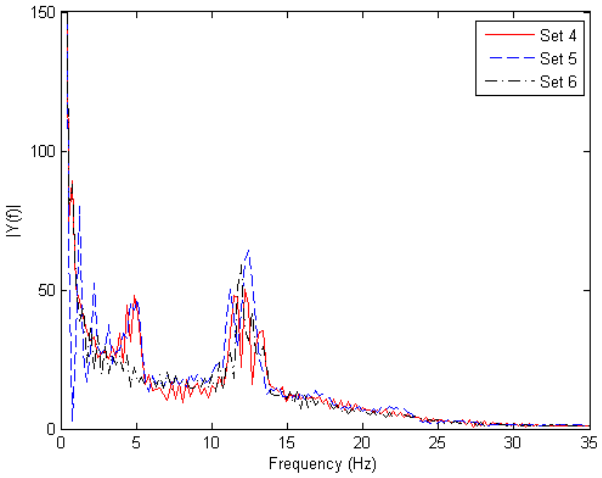

Fig. 15. Sets 4, 5, and 8 FFT

TABLE IV
RANKED DATA SETS

Set	Tire Pressure (psi)	Spring (lb/in)	Damper Setting
1	12	350	Full Soft
5	6	200	Full Stiff
3	6	350	Full Soft
2	8	350	Full Soft
7	6	550	Full Soft
6	6	200	Full Soft
8	6	550	Full Stiff
4	6	350	Full Stiff

Figures 12 – 15 indicate that a large frequency component to the torque oscillations is 12 - 13 Hz. It is believed that this peak is due to the tire/spring/damper system. Comparing Figures 14 and 15 indicates that when the damper setting is switched from full soft to full stiff, an additional peak in the FFT plot at around 5 Hz appears and the peak at 12 – 13 Hz has diminished slightly. The ranked data in Table IV shows that, in general, sets where the damper was set to full soft performed better than sets with the damper set to full stiff (with the exception of set 5). One possible explanation for this is that the tire is able to dampen out torque oscillations at higher frequencies better than at lower frequencies. The lower the frequency of the input torque, the longer the tire has to react to the oscillation and make a corresponding change in torque applied to the ground. The higher the frequency of the input torque, the better the tire is able to effectively average out the oscillation and provide a more steady delivery of torque to the ground. It appears that higher tire pressures may result in more torque put to the ground, but there is insufficient data to support this. Additionally, there does not seem to be any correlation in spring rate and the results in Table IV.

Conclusion

Now that transient loading of the drivetrain has been obtained, it will be incorporated into fatigue life estimates to improve component design. This will be done through a rainflow cycle count program to calculate stress ratios and number of cycles. A correlation was found between damper settings and acceleration performance; however, it is not conclusive since vehicle parameters such as tire temperature were not held completely constant between each run. In order to better compare torsion bridge data and vehicle parameters such as longitudinal acceleration, wheel speeds, and damper position which are logged on the vehicle's data acquisition unit, these tests should be repeated with the torsion bridge data fed directly to the vehicle's data logger via a slip ring. This will allow for torque data to be displayed side-by-side with all other vehicle parameters. Additionally, run times specifically within the traction limited section would provide another method for evaluating the effect of each vehicle setting.

Acknowledgements

The author would like to thank Huy Nguyen at Diversified Technical Systems, Inc. for arranging the sponsorship of the loaner SLICE NANO unit that was used for data acquisition during these tests.

Also special thanks to: Max Koessick, John Meek, Karl Scherer, and Santiago Ruiz at Sikorsky Aircraft for the installation of the torsion bridges and technical assistance in the implementation, execution, and analysis of these tests.

References

[1] D. T. Systems, "SLICE MICRO and SLICE NANO," [Online]. Available: http://dtsweb.com/library/esensing/DTS_Datasheet-SLICE_NANO_MICRO_2016-03.pdf. [Accessed 1 2017].